EMERGING STRUCTURE OF THE NICOTINIC ACETYLCHOLINE RECEPTORS

Arthur Karlin

The conversion of acetylcholine binding into ion conduction across the membrane is becoming more clearly understood in terms of the structure of the receptor and its transitions. A high-resolution structure of a protein that is homologous to the extracellular domain of the receptor has revealed the binding sites and subunit interfaces in great detail. Although the structures of the membrane and cytoplasmic domains are less well determined, the channel lining and the determinants of selectivity have been mapped. The location and structure of the gates, and the coupling between binding sites and gates, remain to be established.

ION CHANNEL STRUCTURE

CURARE
A poisonous extract from certain tropical vines, which blocks neuromuscular transmission, causing relaxation and paralysis. The active component in curare is (+)-tubocurarine.

The nicotinic acetylcholine (ACh) receptors have been objects of attention since Claude Bernard investigated the action of a Central American arrow poison (CURARE). The 'nicotinic receptive substance' in the neuromuscular junction was the first receptor to be recognized and named[1], the first to be studied electrophysiologically[2], and the first to be characterized biochemically. The subunits were identified and cloned, and the ACh-binding sites and the channel-lining residues were mapped in the subunit sequences. The shape of the complex, the arrangement of its subunits, and some secondary structural features, were visualized by electron microscopy. The threading of the subunits through the membrane, and their arrangement around the central channel were determined. Single-channel recording cut its teeth on these channels, and many models were developed to fit the kinetics of agonist binding, channel opening and closing, and desensitization. Although the requirement for a conformational change that links ACh binding to channel opening has been obvious, the details have remained elusive. The *sine qua non* for success is a high-resolution structure.

In a surprising manner, this structure has now become available for the extracellular domain. The recently solved structure of a homologous protein — a snail ACh-binding protein (AChBP) — that few knew existed a year ago is both beautiful and enlightening. Although crystallized in the absence of specific ligand, the structure of the site that binds ACh and curare in this protein is clear. In another surprising development, a tight complex of a designer receptor fragment and α-bungarotoxin was crystallized, and the structure related to that of the ACh-binding protein. The result is that the mode of binding of curare-like polypeptide snake toxins to the receptor has also become much clearer.

Although the detailed structure of the membrane domain eludes us, the framework provided by electron microscopy and spectroscopic methods, and the constraints provided by chemical probes and the effects of mutagenesis, provide a picture of the channel and its selectivity filter and gates. Furthermore, the picture is dynamic. Many residues that line the channel, that are associated with the gates and even with the protein–lipid interface, are in different environments in the different functional states.

Here, I review our current knowledge of the structure of the extracellular and membrane domains of the nicotinic receptors. These receptors also have a large cytoplasmic loop that is involved in receptor biosynthesis, assembly, transport, clustering, anchoring and modulation, but its structure is outside the scope of this review.

Center for Molecular Recognition, and Departments of Biochemistry and Molecular Biophysics, Physiology and Cellular Biophysics, and Neurology, Columbia University, New York, New York 10032, USA.
e-mail: ak12@columbia.edu
DOI: 10.1038/nrn731

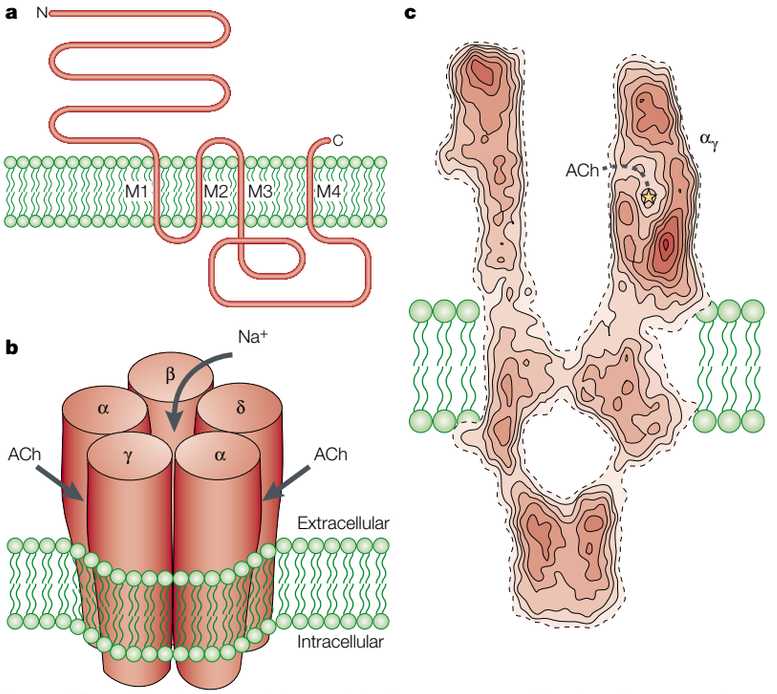

Figure 1 | **Structure of the nicotinic acetylcholine receptors. a** | The threading pattern of receptor subunits through the membrane. **b** | A schematic representation of the quaternary structure, showing the arrangement of the subunits in the muscle-type receptor, the location of the two acetylcholine (ACh)-binding sites (between an α- and a γ-subunit, and an α- and a δ-subunit), and the axial cation-conducting channel. **c** | A cross-section through the 4.6-Å structure of the receptor determined by electron microscopy of tubular crystals of *Torpedo* membrane embedded in ice. Dashed line indicates proposed path to binding site. Part **c** reproduced with permission from REF. 22 © 1999 Academic Press.

Cys-loop receptors

The nicotinic ACh receptors belong to a superfamily of ligand-gated ion channels, known as Cys-loop receptors because all family subunits contain in their amino-terminal, extracellular halves a pair of disulphide-bonded cysteines, which are separated by 13 residues[3–6]. The superfamily includes muscle-type and neuronal-type nicotinic ACh receptors, 5-hydroxytryptamine type 3 (5-HT_3) receptors, γ-aminobutyric acid type A ($GABA_A$) and $GABA_C$ receptors, glycine receptors, and invertebrate glutamate[7] and histidine[8] receptors. The sequences and HYDROPATHY PLOTS of all of the subunits are similar, and the threading of the subunits through the membrane, which was determined in the *Torpedo californica* ACh receptor[4], is presumably also the same (FIG. 1a).

There are five classes of muscle-type ACh receptor subunit: α1, β1, γ, ε and δ. In ELECTROCYTES[9] and fetal muscle, the receptor composition is $(\alpha1)_2\beta1\gamma\delta$, whereas in adult muscle[10], the composition is $(\alpha1)_2\beta1\varepsilon\delta$. There are 12 known types of vertebrate neuronal ACh receptor subunit: α2–α10 and β2–β4. When expressed heterologously, α7, α8 and α9 can form functional homopentamers[11–14]. By contrast, the α2–α6 and α10 neuronal subunits form functional complexes only when co-expressed with β-subunits or with other α-subunits[15–18]. In the muscle-type ACh receptor[19], the subunits are arranged in the circular order of αγαβδ (FIG. 1b), like barrel staves around a central channel[20–22] (FIG. 1c).

Function

Four functional states have been described in ACh receptors: the resting (closed) state, the open state, the fast-onset desensitized (closed) state, and the slow-onset desensitized (closed) state[2,23–33] (FIG. 2). The resting state is the most stable state in the absence of agonist, and the slow-onset desensitized state is the most stable state in the presence of agonist. The open state and the fast-onset desensitized state are metastable states, in that their concentrations rise transiently and reach a very low value at equilibrium. The role of desensitization in cholinergic neurotransmission under normal physiological conditions is uncertain, but is evident both in some pathological conditions and in neurotransmission by other neurotransmitters[34].

ACh receptors are ALLOSTERIC, in that they are oligomeric, contain multiple agonist-binding sites, non-competitive-antagonist sites, and gates that interact at a distance through changes in the quaternary structure of the receptor. They also open, albeit rarely, and desensitize in the absence of agonist. Their behaviour can therefore be described by the MONOD–WYMAN–CHANGEUX (MWC) MODEL of allosteric interactions[35–37]. Constrained by the postulated lower free energy of symmetrical subunit interactions, state changes were associated exclusively with concerted, symmetry-preserving transitions of the subunits. Most ACh receptors, however, are asymmetrical heteromers, in which neither the ACh-binding sites nor the subunit–subunit interfaces are identical (see below). The MWC theory has been extended to accommodate multiple functional states and quasi-symmetry. It provides an adaptable and heuristic rationalization of most[29,33], although not all[31,38,39], receptor phenomenology.

Structure of the extracellular domain

Our knowledge of the structures of the extracellular domains of all Cys-loop receptors, and particularly of the nicotinic ACh receptors, took a giant step forward with the solution of the high-resolution structure of the AChBP (see Protein Data Bank (PDB) entry 1I9B) from *Lymnaea stagnalis*[40]. AChBP is a homopentameric, soluble protein that is secreted by snail glial cells into cholinergic synapses, where it modulates synaptic transmission by binding ACh[41]. AChBP binds agonists and competitive antagonists of the nicotinic ACh receptor, including ACh, nicotine, epibatidine, (+)-tubocurarine and α-bungarotoxin. The spectrum of affinities resembles that of homomeric neuronal nicotinic receptors that are composed of α7- or α9-subunits. The structure of AChBP reveals much about the nature of the ligand-binding domains and the subunit interfaces of its cousins, the nicotinic receptors.

The AChBP subunit, which was detected originally in a snail complementary-DNA library, contains 210 amino acids and is 20–24% identical to aligned sequences of the amino-terminal, extracellular halves of nicotinic ACh receptor subunits, and 15–18% identical to similarly aligned sequences of the 5-HT_3, $GABA_A$, $GABA_C$ and glycine receptor subunits. The eponymous disulphide-bonded cysteines are present in the AChBP subunit, but there are only 12 intervening residues in

HYDROPATHY PLOT
A plot that allows the visualization of hydrophobicity patterns in a peptide sequence, and is particularly useful in determining the membrane-spanning regions of proteins. Obtaining a plot requires the use of a hydropathy scale that is based on the hydrophobic and hydrophilic properties of the 20 amino acids. A moving window determines the summed hydropathy at each point in the sequence, and this value is then plotted against the amino-acid positions.

ELECTROCYTE
A generic name for the cells of the electric organ of electric fish.

ALLOSTERIC
A term used to describe proteins that have two or more binding sites, in which the occupancy of each site affects the affinities of the others.

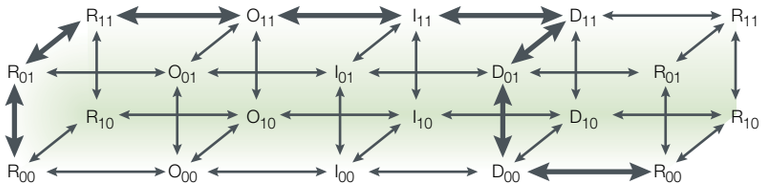

Figure 2 | **Transitions between the four states of the ACh receptor.** The states of the acetylcholine (ACh) receptor are resting (R), open (O), fast-onset desensitized (I), and slow-onset desensitized (D). It is assumed that the two agonist-binding sites are different. The subscripts indicate the state of occupation of the sites: 00, unoccupied; 01 or 10, singly occupied; 11, doubly occupied. It is assumed that the resting state and the desensitized states are directly connected by allowed transitions. Heavy arrows indicate a principal reaction pathway.

place of the 13 that are found in the Cys-loop receptor subunits. These residues are almost all different in AChBP compared with Cys-loop receptor subunits. It is possible that this conserved loop participates in coupling the extracellular domain of Cys-loop receptors to the membrane domain that is absent in the AChBP.

MONOD–WYMAN–CHANGEUX MODEL
A model that is used to describe the nature of allosteric interactions in oligomeric proteins. It requires the protomers to be associated such that all of them have equivalent positions. The protomers must exist in two forms — tense (ligand-free) and relaxed (ligand-bound) — that are in equilibrium. Ligand binding causes a concerted change in the protomers, and the binding curve for an allosteric protein can then be calculated from the so-called allosteric constant, which depends on the ratio between the tense and the relaxed forms and their dissociation constants.

3_{10} HELIX
A structural feature that consists of three amino-acid residues per turn, and a 2-Å helix translation per residue.

CRYO-ELECTRON MICROSCOPY
A microscopy method in which the specimen of interest is suspended in buffer, sprayed on a copper mesh, and dipped into an extremely cold liquid such as liquid ethane. The extremely cold temperature turns the buffer into a layer of ice, trapping the specimen inside it. The advantage of this method is that the specimen is largely preserved in its native state.

AFFINITY LABELLING
A method for labelling the functional parts of a protein, such as a receptor, by covalently linking a tagged agonist, antagonist or other molecule that the protein normally binds.

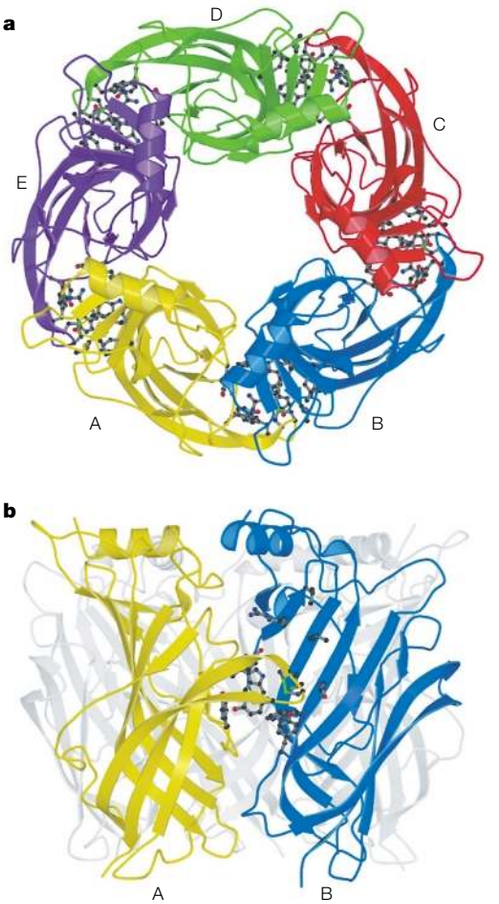

Figure 3 | **The acetylcholine-binding protein. a** | The acetylcholine-binding protein (AChBP) viewed down the fivefold axis. Each of the five identical subunits is rendered in a different colour and labelled A, B, C, D or E. A ligand-binding site is formed at each interface, with A forming the (+) side and B forming the (–) side, and so on for B–C, C–D, D–E and E–A. **b** | The view perpendicular to the fivefold axis, showing one ligand-binding site as a ball-and-stick representation. Reproduced with permission from REF. 40 © 2001 Macmillan Magazines Ltd.

In three dimensions, the AChBP is a cylinder that is 80 Å in diameter and 62 Å in height (FIG. 3). Each of the five identical subunits occupies a sector of the cylinder, and, together, the subunits line an axial channel that is 18 Å in diameter. In face view, the structure resembles a 'windmill toy' with five blades. The subunits start at their amino termini with a three-turn α-helix, and thereafter form ten β-strands and connecting loops, including two short 3_{10} HELICES. The β-strands are arranged with a uniquely modified immunoglobulin-like topology. In three dimensions, the Cys-loop is close to the subunit carboxyl terminus at the 'bottom' of the cylindrical complex. In the aligned Cys-loop receptor subunits, the sequences continue immediately into the membrane-spanning domain M1; so, in the receptors, the Cys-loop and the bottom of the complex are close to the extracellular surface of the membrane. The amino terminus of the AChBP subunit is at the opposite end of the cylinder (the 'top'), placing the amino termini of the Cys-loop receptor subunits farthest from the membrane. The main immunogenic region of the ACh receptor α1-subunit[42] aligns with AChBP residues at the top of the cylinder. The secondary structure of the AChBP subunit closely resembles that predicted for the extracellular domain of the ACh receptor subunits[43].

The extracellular domain of *Torpedo* ACh receptors, obtained by CRYO-ELECTRON MICROSCOPY (FIG. 1c), is similar in size and shape to the structure of AChBP, and also contains twisted β-strands[22]. The proposed features of a tunnel that leads from the channel vestibule to the binding site (the dotted line in FIG. 1c), and of a passage through the wall from the periphery to the vestibule[22], are not present in the AChBP structure[40].

Brejc and co-workers mapped the contact residues (FIG. 4) in the subunit–subunit interfaces of the AChBP, and noted that they were poorly conserved among the Cys-loop receptor subunits[40]. However, a lack of conservation among different subunits is to be expected, because different contact residues would be needed to obtain specific arrangements of the subunits in heteropentameric Cys-loop receptors[44].

ACh-binding sites

Contributions of the α-subunit. AFFINITY LABELLING of the ACh-binding site led to the first identification of a receptor subunit — the electrocyte ACh receptor α-subunit[45]. The muscle-type ACh receptor has two ACh-binding sites per $(\alpha1)_2\beta1\gamma\delta$ complex, corresponding to the two α-subunits[9]. The affinity-labelled residues are a pair of adjacent cysteines, αCys192 (bp187) and αCys193 (bp188)[46], which form a highly unusual disulphide bond[3] (FIG. 4). (The numbers of the residues correspond to the mature *Torpedo* α-subunit and are followed by the numbers of the aligned residues in AChBP, preceded by 'bp'.) These adjacent cysteines are characteristic of all ACh receptor α-subunits. Subsequently, four widely spaced aromatic residues — αTyr93 (bpTyr89), αTrp149 (bpTrp143), αTyr190 (bpTyr185) and αTyr198 (bpTyr192) — were affinity labelled[47,48]. These aromatic residues are conserved in all ACh receptor α-subunits, except in neuronal α5, in which Asp190 replaces Tyr190.

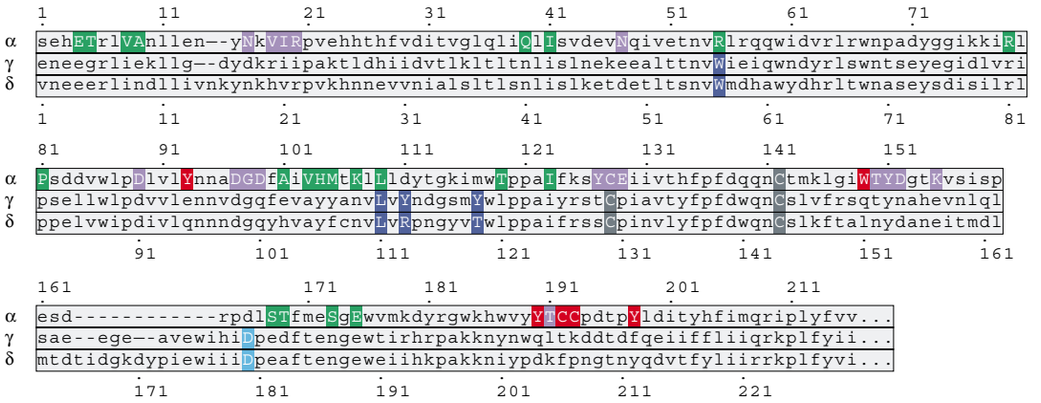

Figure 4 | **Aligned sequences of the extracellular domains of the *Torpedo californica* ACh receptor α-, γ-, and δ-subunits.** Residues of the acetylcholine (ACh) receptor that are aligned with the residues that line the binding site of the ACh-binding protein (AChBP) are underlined. Those on the (+) side of the binding site of the α-subunit are in red; those on the (–) side of the binding sites of the γ- and δ-subunits are in dark blue. Also, by alignment with the AChBP, the residues in the α-subunit that form the subunit–subunit interfaces on the (+) side are in violet, and those on the (–) side are in green. Presumably, aligned residues in the other subunits contribute in a similar manner to subunit–subunit interactions. δAsp180, which is known to be close to αCys192/193 in *Torpedo*, and the aligned γAsp174, are in light blue. The cysteines in the 15-residue loop are in grey. The membrane-spanning M1 segment is predicted to begin at αPro211. The β-subunit sequence, which does not contribute to a binding site, is omitted.

Contributions of γ- (ε-) and δ-subunits. Neighbouring subunits also contribute to the ACh-binding site. Heterologous expression of muscle-type α1-subunits alone did not yield ACh-binding sites. However, ACh-binding sites were generated by co-expression of α1 with the γ- or δ-subunit, but not with the β-subunit[49–52]. Labelling and cross-linking provided evidence that the ACh-binding sites are in the interface between subunits. (+)-Tubocurarine specifically photolabelled the aligned pairs γTrp53 (bpTrp53) and δTrp55, and γTyr111 (bpVal106) and δArg113, as well as γTyr117 (bpLeu112) (FIG. 4). Another photoactivatable competitive inhibitor, benzoylbenzoylcholine, photolabelled the aligned pairs γLeu109 (bpArg104) and δLeu111 (REF. 53). The identification of carboxylate residues in the vicinity of the binding site, and a constraint on the distance between the ACh-binding site in the α-subunit and an adjacent subunit, were obtained with a 9-Å-long bifunctional reagent that cross-linked reduced αCys192/193 to δAsp180 (bpAsp161)[54].

COREY–PAULING–KOLTUN REPRESENTATION
A space-filling atomic model in which the atoms are represented as spheres, the radii of which are proportional to the van der Waals radius of the atom.

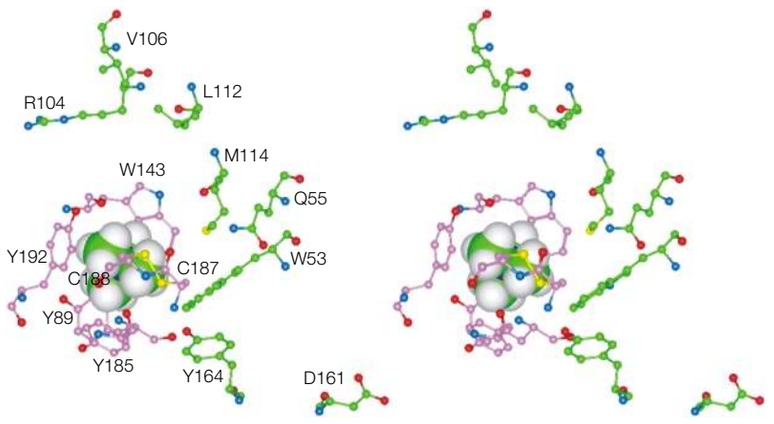

Figure 5 | **The binding site of AChBP.** Residues of the acetylcholine-binding protein (AChBP) that are in or close to the binding site are shown as a ball-and-stick representation. The carbon atoms of the residues from the (+) side of the subunit interface are coloured pink, and those from the (–) side are coloured green. Nitrogens are blue, oxygens are red, and sulphurs are yellow. A molecule of tetramethylammonium in COREY–PAULING–KOLTUN (CPK) REPRESENTATION is placed approximately in the middle of the aromatic side chains, avoiding any overlaps with residue atoms. The pictures are in stereo. Modified with permission from REF. 40 © 2001 Macmillan Magazines Ltd.

ACh-binding site in AChBP. All of the residues that are associated with the binding sites in the α-, γ- and δ-subunits are conserved in AChBP, and all of these conserved residues, except for bpAsp161, line a cavity that undoubtedly contains the ACh-binding site[40] (FIG. 5). The AChBP binding-site residues that align with the α-subunit binding-site residues are on one side of AChBP (the (+) side), and the residues that align with the γ- and δ-binding-site residues are on the opposite (–) side. The residues on the (+) side are in loops between β-strands, whereas those on the (–) side are mostly within β-strands. As has been long held[55,56], the ACh-binding sites in the ACh receptors are also interfacial, contrary to the proposal that they are completely buried in the α-subunits[22] (FIG. 1c).

The AChBP binding site opens to the outside of the cylindrical complex, about midway between its top and bottom (FIG. 3b). There is no opening of the binding site to the axial channel, such as has been proposed in the ACh receptor[22,57]. Viewed from the top of the cylinder, the (–) sides of each AChBP binding site are anticlockwise to the (+) side (FIG. 3a). In muscle-type receptors, the (–) sides of the ACh-binding sites are contributed by the γ- (or ε-) and δ-subunits. Therefore, the muscle-type subunits, previously shown to form a circle around the central channel in the order αγαδβ (REF. 19), must be in an anticlockwise arrangement, as viewed from the synaptic cleft[40] (FIG. 1).

Although the AChBP was crystallized in the absence of a specific binding-site ligand, AChBP did contain a molecule of *N*-2-hydroxyethylpiperazine-*N*′-2-ethanesulphonate (HEPES) in the binding-site cavity. HEPES has a very low affinity for the AChBP, but was present at ~100 mM in the crystallization buffer. Both of the two potentially protonated and positively charged nitrogens

CATION–π INTERACTION
A non-covalent interaction between a cation and the face of an aromatic ring.

QUATERNARY AMMONIUM ION
An ammonium ion in which the nitrogen is bonded to four carbons.

EC_{50}
The concentration of agonist that evokes a half-maximal response.

of the piperazine ring are close to the rings of bpTrp143, within a cage of six aromatic side chains. This arrangement is consistent with the important contribution of CATION–π INTERACTIONS to the binding of QUATERNARY AMMONIUM IONS[58,59].

Quaternary ammonium binding by the ACh receptor. Agonists and competitive antagonists of the ACh receptor have at least one quaternary ammonium group or a protonated tertiary ammonium group. The simplest agonist, tetramethylammonium, consists of only a quaternary ammonium group. It seems likely that in the ACh receptor, the ammonium group binds in the cage of five aromatic side chains that are aligned with bpTyr89, bpTrp143, bpTyr185 and bpTyr192 from the (+) side, and bpTrp53 from the (–) side (FIG. 5).

A sixth aromatic side chain in the (–) side of AChBP, bpTyr164, is not conserved in the ACh receptor γ- and δ-subunits, but two or three negatively charged side chains at the aligned position and close by — including γAsp174 and δAsp180, aligned with bpAsp161 — are completely conserved. Replacing δAsp180 or the aligned γAsp174 with asparagine decreased the apparent affinities for agonists by 100–200-fold, and the affinities for competitive antagonists by 10–15-fold[60]. However, mutation of the aligned εAsp175 in the $\alpha_2\beta\varepsilon\delta$ complex affected the transduction of agonist binding into channel opening (that is, gating), rather than agonist binding *per se*[61].

These negatively charged residues are the probable sources of the negative electrostatic potential in the ACh-binding site of the receptor[60–63], and their movement towards a bound quaternary ammonium group could be part of the activation mechanism[64].

The location of the quaternary ammonium group within the cage of aromatic side chains is consistent with receptor activation by tethered agonists, namely quaternary ammonium moieties that are attached to αCys192/193 (REF. 64), and at the positions of αTrp149 (REF. 58) and αTyr198 (REF. 65). In addition, ACh mustard, in which the quaternary ammonium group itself reacts, labelled αTyr93 (REF. 66).

Structural changes of the binding site. In general, ACh receptor agonists are smaller than competitive antagonists. In addition, affinity labels that were attached to reduced αCys192/193 and acted as tethered agonists were at most 9-Å long, whereas affinity labels that acted as tethered antagonists were at least 12-Å long. This is consistent with the idea that the ACh-binding site contracts around a bound agonist and less so around a bound antagonist[64], similar to what occurs in the binding core of the AMPA (α-amino-3-hydroxy-5-methyl-4-isoxazole propionic acid)-type glutamate receptor GluR2 (see PDB entry 1FTO)[67].

An indication of an agonist-induced structural change is that the disulphide bond between αCys192 and αCys193 is much less susceptible to reduction by dithiothreitol in the presence of agonists than in the presence of competitive antagonists, and the more effective the agonist, the more complete the protection[68]. The structure of AChBP provides a rationale for this result, in that the disulphide faces into the binding-site crevice at the tip of the loop that is a loose lid on the binding-site cavity (FIGS 3 and 5). As Brejc and co-workers pointed out, the loop would have to move for a large antagonist to enter the site. It is possible that when the site is unoccupied, or when it is occupied by antagonist, the loop with the disulphide is mobile and accessible. However, when an agonist occupies the site, the loop might be immobilized, the binding site capped, and the disulphide inaccessible even to a relatively small molecule such as dithiothreitol. If the 'lid-shut' conformation corresponds to the active state of the binding site, which is coupled to the open state of the channel, the closed lid could explain the 2,500-times slower dissociation of agonist from the open state of the receptor than from the resting state[33].

If this general view of activation at the binding site is valid, then some competitive antagonists also alter the structure of the binding site, not enough to activate adult receptors, but enough to activate fetal receptors[69], and chemically[64] or genetically altered[70] receptors.

Mutations at the binding site. Mutations of residues that contact the ligand would be expected to alter binding. However, not all residues in which mutation alters apparent or actual binding contact the ligand. Mutations of residues that are far from the ACh-binding sites alter the EC_{50} or equilibrium binding constants. Mutations of α-subunit residues that are established to be within the ACh-binding site — αCys192/193 (REF. 71), αTyr93 (REFS 61,72,73), αTrp149 (REF. 72), αTyr190 (REFS 72–75) and αTyr198 (REFS 74,75) — affected agonist binding or gating, and also the binding of competitive antagonists. A kinetic analysis[61] showed that the mutation of αTyr198 to phenylalanine affected gating, but not the affinity for ACh. Mutations of γTrp55 and δTrp57 affected agonist binding or gating, but had little effect on antagonist binding[76]. Given that the movements of the residues that contact agonist are likely to be involved in the transduction of binding into gating, effects of mutations on both binding and gating, or principally one or the other, are not difficult to rationalize.

By contrast, mutations of the ACh receptor residues γTyr111 and δArg113 (bpVal106)[77,78], γTyr117 and δThr119 (bpLeu112)[52], and γLeu119 (bpMet114)[79], affected competitive antagonist binding, but not agonist binding or gating. In AChBP, the three residues at 106, 112 and 114, together with Arg104, form the top of the binding-site cavity (FIG. 5). AChBP Arg104 aligns with γLeu109 and δLeu111, which were photolabelled by the competitive antagonist benzoylbenzoylcholine[53]. These residues in the γ- and δ-subunits are also likely to form the top of the binding site and to interact with bulky competitive antagonists, but not with agonists.

Binding-site non-equivalence. In the muscle-type ACh receptor, the two ACh-binding sites are different. This was apparent in the much greater rate of reaction of 4-(*N*-maleimido)benzyltrimethylammonium with one of the two ACh-binding sites in the *Torpedo* receptor[80], probably the αγ site[60]. In heterologously expressed combinations of subunits, the complex of α- and

γ-subunits had a higher affinity for competitive antagonists, whereas the complex of α- and δ-subunits had a higher affinity for agonists[50]. In complete receptor complexes, the two sites also bind agonists with different affinity[31], and structural differences in the αγ, αε and αδ sites were detected with a fluorescent agonist[81]. (+)-Tubocurarine and conotoxin MI bind much more tightly to the αγ site than to the αδ site; the differences are partly due to γTyr111 and the aligned δArg113 (REF. 78). Waglerin 1 is a 22-residue-polypeptide snake toxin that binds orders of magnitude more tightly to the αε binding site of the adult mouse receptor than to the αδ binding site[82,83]. *Naja mossambica mossambica I* α-neurotoxin binds 1,000 times more tightly to the αγ and αδ sites than to the αε site[84]. Despite this evidence for non-equivalence, kinetic models that assume equivalent binding sites, as well as models that assume non-equivalent sites, have been used successfully to fit ACh receptor function under different conditions[31,33,85].

Polypeptide-snake-toxin binding sites

α-Neurotoxins. The α-neurotoxins in the venoms of elapid and hydrophid snakes are high-affinity competitive inhibitors of ACh binding to nicotinic ACh receptors in striated muscle[86]. The α-neurotoxins, of which α-bungarotoxin is the most potent example, have been indispensable tools in the characterization of ACh receptors[87,88]. The α-neurotoxins are members of the 'three-finger' protein family[89]. There are 'short' and 'long' toxins, which differ in length by about ten residues. Short α-neurotoxins (for example, erabutoxin) contain three loops or 'fingers' that extend from a globular core, cross-linked by four disulphide bonds. Long α-neurotoxins (for example, α-bungarotoxin) are structurally similar to the short toxins, but include a fifth disulphide bond in finger 2, and a carboxy-terminal tail.

α-Subunit fragments. One approach to studying the structure of the toxin–receptor complex is based on the binding of α-bungarotoxin by α1 alone[90], and by fragments of α1 (REFS 91–93). These fragments, one as short as 12 residues, all include the invariant α-subunit motif Tyr190–X191–Cys192–Cys193 (FIG. 4). They bind toxin with affinities that are orders of magnitude lower than that of the intact receptor complex; this is not surprising, considering that the fragments contain only three of the six key residues in the α-subunit, and none of the key residues in the γ- and δ-subunits, that line the ACh-binding site. Nevertheless, this approach has led to a remarkable breakthrough in our understanding of toxin binding.

A lead peptide, selected for α-bungarotoxin binding from a phage-display library, was modified to decrease the dissociation constant for its complex with toxin to 2 nM (by two orders of magnitude). This figure is within the range of dissociation constants (0.01–10 nM) for the binding of toxin by intact receptors[94]. This 13-mer high-affinity peptide (HAP), aligns (with a gap) with *Torpedo* α187–200, and includes six identical residues and two more residues — Ser192 and Ser193 (*Torpedo* numbering) — that are conservative substitutes for Cys192 and Cys193.

Crystal structure of the peptide–toxin complex. Harel and co-workers[94] crystallized the α-bungarotoxin–HAP complex, and solved its structure to a resolution of 1.8 Å (see PDB entry 1HC9). The bound HAP formed a β-hairpin that superposes on the structure of the corresponding segment in the snail AChBP. This AChBP segment is one of the loops that line the ACh-binding site, and contains the binding-site motif Tyr–X–Cys–Cys.

The crystal structure shows that HAP fits snugly into α-bungarotoxin, contacting fingers 1 and 2 and the carboxy-terminal tail. Most of the residues that have been implicated in the binding of both long and short α-neurotoxins are in finger 2, with which HAP makes the shortest and most numerous contacts. Two invariant residues in finger 2 — Asp30 and Arg36 — make close contact with HAP residues Tyr190, Ser192 and Ser193. In addition, HAP Tyr189, just before Tyr190–X–Ser–Ser, makes two hydrogen bonds from its hydroxyl group to HAP residues. Receptors that bind α-bungarotoxin with high affinity have either tyrosine or phenylalanine at position α189; substitution of non-aromatic residues at this position can prevent binding[94,95].

Modelling AChBP–toxin and receptor–toxin complexes. Because of the exact structural overlap of the first 12 residues of HAP with residues 182–193 of the AChBP, the structure of the HAP–α-bungarotoxin complex can be superposed on the structure of the AChBP, providing a model of toxin binding to the whole protein. By homology, this superposition model reveals the probable mode of α-bungarotoxin binding to ACh receptors. In the model, 18% (760 Å^2) of the accessible surface of the free toxin is buried in the binding site. The bulbous tip of toxin loop 2 seems to be stuck in the binding-site cavity between adjacent subunits. The rest of the toxin extends radially from the outside of the cylindrical pentamer, away from the axis.

As in the complex with HAP, in the homology model, the invariant toxin residues Asp30 and Arg36 are close to the ACh-binding-site residues Tyr190, Cys192 and Cys193. AChBP residues that correspond to receptor residues δ36–38 and δ181–184, on the complementary side of the inter-subunit interface, also contact the toxin. The positively charged toxin residue Lys38 is close to the negatively charged bpAsp161, the equivalent of receptor γAsp174 and δAsp180, which participate in ACh binding[60]. Other evidence indicates that some charged residues in the toxin interact with uncharged residues in the receptor, and vice versa[84].

There are subtleties in the binding of the various α-neurotoxins that are not settled by the homology model. The short and long α-neurotoxins have a core of identical residues that are involved in binding to receptors, but each type has some unique residues that are involved in binding[96,97]. So, the dispositions in the binding site of the short and long toxins are not identical.

SCAM applied to the toxin-binding site. Even with toxin in the binding site, there is still some 'wiggle' room. The toxin-binding site has been studied by the substituted-cysteine accessibility method (SCAM; see below and

Box 1 | **The substituted-cysteine accessibility method**

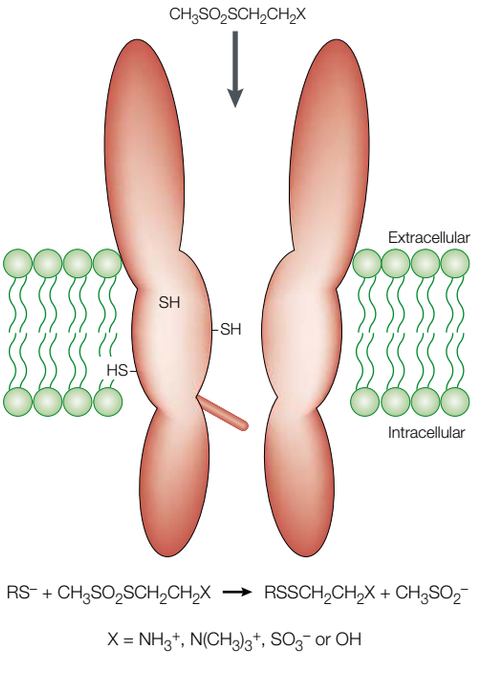

The substituted-cysteine accessibility method (SCAM) is an approach to the characterization of channel[101,131,163] and binding-site structures[62,164,165] that probes the environment of any residue by mutating it to cysteine, and by characterizing the reaction of the cysteine with sulphydryl-specific reagents. Among these reagents, the methanethiosulphonates are attractive because of their small size and their specificity for sulphydryls[166]. The reactions of charged and polar methanethiosulphonates, such as those shown in the figure, are directed to cysteines at the water-accessible surface of proteins, both because of the hydrophilicity of the reagent and because these reagents react at least ten orders of magnitude faster with ionized thiolates than with unionized thiols[167]. Cysteines that substitute for residues in the membrane-embedded segments of a channel protein are either buried in the protein interior, exposed to lipid, or exposed to water (see figure). It is assumed that the only water-accessible residues in the membrane domain are exposed to water in the channel lumen. In the case of the acetylcholine (ACh) receptor, the positively charged methanethiosulphonate ethylammonium (MTSEA) and methanethiosulphonate ethyltrimethylammonium (MTSET) are conducted by the open channel[131], and so have access to all exposed residues. The reaction of a methanethiosulphonate with a substituted cysteine in the channel can be sensitively monitored electrophysiologically by the effect of the reaction on ACh-induced current in the heterologously expressed mutant. Fortunately, cysteine substitution is very well tolerated[102,168].

SCAM has been used to identify channel-lining residues, to determine the potentially different environments of these residues in the open and closed states of the channel, to assess secondary structure, to locate selectivity filters and gates, to map the binding sites of channel blockers, and to estimate the electrostatic potential in the channel[163]. These uses require the determination of the reactivity of the cysteines; that is, the reaction rate constant for each cysteine and for each reagent used. The rate constant for the reaction of a given cysteine with a methanethiosulphonate (or other reagent) depends on the intrinsic reactivity of the reagent, on rates of reagent transport to and from the target cysteine, and on the reactivity of the cysteine sulphydryl[132]. Rates of reagent transport depend on steric and electrostatic factors along the pathways and at the reaction site. The reactivity of the target cysteine itself depends on local steric factors and, crucially, on the extent of deprotonation of the cysteine sulphydryl[133]. The individual determinants of the reaction rate can be estimated by taking the ratio of rate constants for reactions that differ only in that one determinant. We located the resting gate in the ACh receptor by taking the ratio of the rate constant for the reaction of MTSEA added to one side of the membrane to the rate constant for the reagent added to the other side, for a sequence of substituted cysteines that spanned the gating region[123]. We have also estimated the intrinsic electrostatic potential at a given cysteine by taking the ratio of the rate constants for the reactions of methanethiosulphonates that differ only in their charge[62,132,133].

These methods allow specific and sensitive probing of femtomolar quantities of heterologously expressed channels in intact cells.

BOX 1). Receptor residues α183–198 have been mutated one at a time to cysteine. Covalent attachment to these cysteines of a number of different moieties (neutral, negatively charged, and even one positively charged) did not block toxin binding. Only the attachment of positively charged quaternary ammonium moieties to the cysteines blocked toxin binding[98]. A similar result was obtained with the cysteine mutant of γLeu119, a residue in the complementary surface of the binding site that interacts with the toxin[79]. The block of toxin binding by the tethered quaternary ammonium moieties might involve conformational changes, as well as steric hindrance[58,64,65].

Membrane domain

Physical approaches. Cryo-electron microscopy of tubular arrays of *Torpedo* receptors in the membrane yielded a 9-Å-resolution map that showed five kinked rods around the central axis of the membrane domain; these were presumed to be helices lining the channel lumen, which was not resolved[21]. No other regular structures were resolved in the membrane domain. Unwin conjectured that the rods were the M2 segments and that the rest of the membrane domain was composed of β-sheet. Infrared spectroscopy of proteolytically shaved, membrane-embedded fragments of receptor was consistent with 50% (REF. 99) or considerably more[100] α-helical secondary structure.

Chemical approaches. The accessibility of channel-lining residues to hydrophilic reagents indicated that ~75% of M2 was α-helical, and that the rest was possibly β-strand[101,102]; however, the amino-terminal third of M1 did not seem to have a regular secondary structure[103,104]. The irregular region of M1, and the β-strand region of M2, might be aligned close to the extracellular surface of the membrane. The pattern of labelling with hydrophobic reagents from the lipid bilayer was consistent with considerable α-helical content in M3 and M4, and non-helical structure in the middle of M1 (REFS 105,106).

Computational methods. Originally, the four predicted membrane-spanning segments were assumed to be α-helical[107–109]. A more refined computational approach, albeit one that was not designed for membrane-embedded segments, did predict that M2 was predominantly α-helical, but that less than half of M1, M3 and M4 was α-helical, and that much of the rest of these segments had a β-strand configuration[43].

Mutational approaches. The periodicity of the functional effects of the substitution of αM4 412–425 by tryptophan was consistent with an α-helical structure[110].

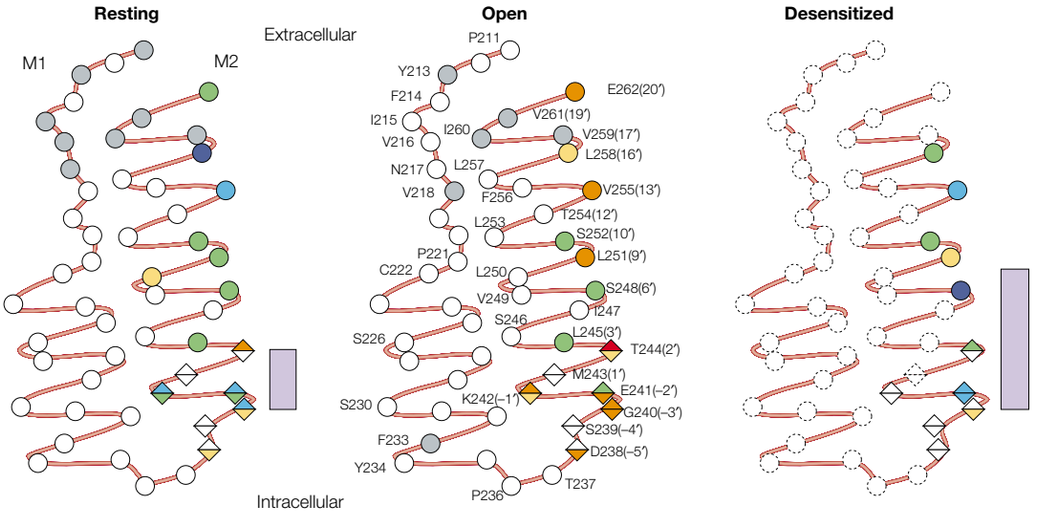

Figure 6 | **M1, M2 and the M1–M2 loop of the mouse muscle ACh receptor.** In this muscle-type acetylcholine (ACh) receptor, M1 is represented as half coil, half α-helix, and M2 is represented as an α-helix. The channel lumen is to the right of each M2 segment. The exposure of M2 is consistent with results obtained by photolabelling with noncompetitive inhibitors, and by the use of the substituted-cysteine accessibility method (SCAM). The upper part of M1 is also exposed in the channel. The rate constants for the reactions of methanethiosulphonate ethylammonium (MTSEA) with the substituted cysteines in the resting state, the open state and the desensitized state were rounded to the nearest power of 10, and colour coded as follows: red, 10^4; orange, 10^3; yellow, 10^2; green, 10^1; light blue, 1; dark blue, 0.1 (units are 1 M^{-1} s^{-1}). Grey indicates a significant reaction, but one in which the rate constant was not determined. White indicates no detectable reaction. Symbols with dotted borders indicate no data. Circles indicate that MTSEA was added extracellularly. Triangles that point extracellularly also indicate the extracellular addition of MTSEA; triangles that point intracellularly indicate the intracellular addition of MTSEA. The violet bars indicate the inferred locations of the gates in the resting and desensitized states[124].

In conclusion, the membrane-spanning segments are not completely α-helical, as originally predicted, but seem to be a mixture of α-helix, β-strand, and irregular secondary structures. The little that is known about the tertiary structure of this region is the approximate arrangement of the membrane-spanning segments relative to the channel lumen and to the lipid bilayer: M2 and some of M1 line the central lumen, and M3 and M4 are in contact with lipid.

Channel

The receptor channel has three functions. It mitigates the energy barrier to ion translocation through a non-polar lipid membrane; it selects among ions[111]; and it opens and closes[112].

The funnel shape of the channel lumen[22] (FIG. 1c) lowers the energy barrier by allowing ions to be surrounded by water even within the low-polarity interior of the receptor protein and lipid bilayer. Only a short section (~6 Å in length) of the channel is narrow enough to force water and a cation to move in single file[113]. The energy barrier in this region can be lowered by interactions of the permeating ion with charged residues and with side-chain and backbone dipoles[114–117]. This narrow section, which is at the cytoplasmic end of the channel, selects for ion charge and size, and determines conductances[118–122]. This region also contains the resting gate[123,124].

Channel lining. The initial indications of the importance of the M2 segments for channel function were the effects on conductance of exchanging M2 segments from bovine and *Torpedo* ACh receptors[125]. The differences in the two species were due to charged residues flanking M2. These were present in each subunit at aligned positions and were postulated to form rings of mostly negatively charged residues: the extracellular ring, at position 20′ counting from the predicted cytoplasmic, amino-terminal end of M2 (FIG. 6); the intermediate ring (M1–M2 loop position –2′); and the cytoplasmic ring (–5′). The inference of their sidedness was made on the basis of the effects of altering the total charge of each ring on the sidedness of Mg^{2+} block[126].

Specific M2 residues that line the channel were photolabelled with the noncompetitive inhibitors chlorpromazine (at 2′, 6′, 9′)[127,128] and triphenylmethylphosphonium (at 6′)[129]. The pattern of labelling was consistent with the exposure in the channel lumen of a stripe of an α-helix. Aligned residues in different subunits were labelled, consistent with the idea of five M2 segments (one from each subunit) surrounding the channel lumen. By contrast, quinacrine azide photolabelled residues at the extracellular end of αM1, specifically in the open state[44,130].

SCAM. Each residue in M1, M2 and the M1–M2 loop, in both the α- and β-subunits, was mutated to cysteine, and the mutants were tested for reactivity towards small, charged sulphydryl-specific methanethiosulphonate reagents, such as methanethiosulphonate ethylammonium (MTSEA)[101–104,131]. This approach, known as SCAM (BOX 1), identifies residues that are exposed to water,

which in the membrane domain include the channel-lining residues. Residues reacted with MTSEA over the entire length of M2 (REFS 101,102) (FIG. 6). The water-accessible residues included all of those in M2 that were photolabelled by channel blockers. In M1, however, only residues in the amino-terminal third were exposed[103,104]. Presumably, five M2 segments at the narrow end of the channel, near the cytoplasmic surface of the membrane, suffice to line the channel; at the wider end of the channel, near the extracellular surface of the membrane, both M1 and M2 segments line the channel.

Channel dynamics. At many positions in M1 and M2, the reactivities of substituted cysteines were different in the resting, open and desensitized states[101–104,124,131,132] (FIG. 6). Not only were many of the reaction rate constants in the open state different from those in the resting and desensitized states, but also some of the rate constants differed in the resting compared with the desensitized state. Many factors can influence reactivity, including a gate between the side of application of the reagent and the target cysteine, local steric hindrance, and the local electrostatic potential and dielectric constant. The last two influence the local concentration of charged reagents, and the ionization of the unreactive cysteine thiol to the reactive thiolate form. The presence of gates[123,124] and changes in local electrostatic potential[132,133] can be determined (see below), but it is not straightforward to infer the structural basis of widely different reactivities and changes in reactivity in neighbouring residues. Obviously, there are structural changes in the channel concomitant with transitions between functional states, and only some of them involve the gate structure *per se*. Structural changes in the membrane-spanning segments are required to couple agonist binding to the gate, and one specific suggestion arising from the opposite changes in accessibility of cysteine-substituted residues in M1 and M2 is that these two segments slide past each other during gating[4].

The rates of photolabelling by chlorpromazine[134], by quinacrine azide[130,135], and by a hydrophobic photolabel, 3-trifluoromethyl-3-(*m*-iodophenyl)diazirine[136,137], were also state dependent, related to the state-dependent binding of noncompetitive inhibitors, and to state-dependent changes in accessibility and reactivity of the target residues.

The effects of mutations of channel-lining residues, (for example, at M2 9′ and 13′)[70,101,138–141], on opening and closing rate constants, and on desensitization rates, are consistent with these residues being in different environments in the resting, open and desensitized states. Mutations of residues that are not exposed in the channel also affect gating; for example, in M2 (REF. 142), in the M2–M3 loop[143], in M3 (REF. 144) and in M4 (REFS 110,145). Consistent with the coupling of movement of residues far from the channel lumen to changes in functional state, the lipid environment is important for the stability of functional states and the capacity of the receptor to undergo transitions[146]. Even mutations in the large M3–M4 cytoplasmic loop affect gating[147]. The structural changes that coincide with changes in functional state are widespread.

Such structural changes have been visualized by cryo-electron microscopy of two-dimensional crystalline arrays of membrane-embedded receptors. Most strikingly, kinks in five membrane-spanning rods were inferred to block the channel in the absence of ACh, and to move out of the way within milliseconds after the addition of ACh[148].

Conductance and selectivity

Except for an anion-selective invertebrate ACh receptor[149,150], all known ACh receptors are cation selective, as are 5-HT_3 receptors. All other Cys-loop receptors are anion selective. Cation-selective ACh receptors are permeable to monovalent and divalent cations; permeability increases with monovalent ionic radius and decreases with divalent ionic radius, a manifestation of competing influences of ionic size and charge[151,152]. The permeabilities of monovalent cations in the open channel are proportional to their mobilities in bulk water, but the conductances are not, indicating that permeating cations interact with at least one site in the channel[119]. In muscle-type ACh receptors, the ratio of permeabilities p_{Ca}/p_{Na} is ~0.2 (REF. 151). Some neuronal-type ACh receptors — for example, $(\alpha7)_5$ and $(\alpha9)_5$ — have much higher p_{Ca}/p_{Na} ratios[138,153–155].

Reducing the negative charge of the intermediate ring (–2′) in the muscle-type receptor strongly reduced cation conductance[119,126]. Conductance was less sensitive to alterations in the extracellular and cytoplasmic rings of charge. The conductance ratios and the permeability ratios, particularly of the larger cations, were also changed by mutations at –2′. In neuronal-type $(\alpha7)_5$, the glutamic acid to alanine mutation at position –2′ abolished Ca^{2+} permeability, increased the low but significant p_{Cl}/p_{Na} from 0.05 to 0.1, but did not change p_{Na}/p_K (REF. 138). Some mutations of Leu16′ and Leu17′ in the wider part of the channel also eliminated Ca^{2+} permeability, most likely through structural changes that propagated to the narrow region of the channel.

Mutations of the polar residues at the 2′ position in the muscle-type receptor altered the conductance ratios of monovalent cations. The conductances of the larger cations Rb^+ and Cs^+ were particularly sensitive to the volume of the substituted side chain[118,120]. The conductance ratios were most sensitive to mutations at the 2′ position, which is therefore likely to be in the narrowest part of the channel and constitute part of the selectivity filter. The permeabilities of organic cations were also particularly sensitive to mutations at 2′. These permeabilities decreased with increasing hydrophobicity of the substituted residue[121,156]. Identical substitutions in the different subunits did not have identical effects, a reflection of the asymmetry of the channel wall in muscle-type receptors[156,157].

The charge selectivity of $(\alpha7)_5$ (REF. 122), as well as of the 5-HT_3 receptor[158], was changed from cationic to anionic by a minimum of three changes in the M1–M2 loop and in M2. Two of the changes were in the narrow region: the glutamic acid at –2′ was changed to alanine, eliminating the five negative charges in the intermediate ring, and a proline was inserted between –2′ and –3′

(–2″), lengthening the M1–M2 loop by one residue, as in muscle-type γ- and ε-subunits, and in the subunits of the anion-conducting Cys-loop receptors. A third required change was in the wider part of the channel, where Val13′ was changed to threonine. The substituted residues matched those in the anion-conducting glycine receptor α-subunit. The reverse mutations in the glycine receptor changed its selectivity from anionic to cationic[159]. That anion selectivity requires elimination of the negative charges in the intermediate ring at position –2′, and that this change strongly reduces cation conductance, are evidence for electrostatic contributions to conductance and selectivity. The basis for the effects on charge selectivity of the two other mutations is not obvious.

Channel electrostatics

Electrostatic-potential profiles in the lumen of the ACh receptor channel have been determined experimentally[132] and calculated theoretically[160]. Although the two profiles differ in detail, they each contain a cation-stabilizing well of negative electrostatic potential.

The intrinsic electrostatic potential that arises from fixed and induced charges in the receptor was determined at a transmembrane potential of 0 mV at three positions along the αM2 segment[132]: near its cytoplasmic end at 2′, near its middle at 9′, and near its extracellular end at 16′. The intrinsic electrostatic potential ranged from about –200 mV at 2′ to –25 mV at 16′ in the open channel, and was approximately 100 mV more positive at each position in the closed channel. The determination was made on the basis of a comparison of the rate constants for the reactions of differently charged but otherwise similar methanethiosulphonate reagents with cysteines that substituted for residues that face the channel lumen.

The intrinsic electrostatic potential in the vicinity of 2′ in the open channel is almost entirely due to the intermediate ring of charge at –2′. The magnitude of the negative potential decreased linearly as the negative ring charge was decreased by substituting either glutamine or lysine for glutamic acid, and extrapolated to zero potential at a total ring charge of zero. Similar changes strongly reduced cation conductance[126]. So, the magnitude of the negative intrinsic electrostatic potential in the vicinity of the selectivity filter correlates with the cation conductance.

Gates

Resting gate. Unwin[21,22,148] has proposed that the channel gate was formed midway along the M2 segments (FIG. 1c); specifically, by the interacting side chains of the aligned leucines at the 9′ position. However, the effects of replacing two or more of these leucines at a time were not consistent with their mutual interaction[139,140]. Also, replacing all of the leucines at position 9′ with serine in $(\alpha7)_5$ (REF. 70), or with alanine in the 5-HT_3 receptor[161], resulted in channels that still opened and closed. Furthermore, the results of the application of SCAM to αM2 were inconsistent with a gate on the extracellular side of the 2′ position[101,132]. Similar SCAM results were obtained with the $GABA_A$ receptor[162]. No residues were resolved in Unwin's studies, and SCAM determines sidedness only by accessibility. The two results could be reconciled if there were a vestibule that extends into the membrane domain from the cytoplasmic side.

The gate was located more precisely by applying SCAM to cysteines substituted at positions –4′ to 2′ (REF. 123) (FIG. 6). Positively charged, sulphydryl-specific reagents were applied both intracellularly and extracellularly, and in the open and closed states of the channel, and the rate constants were determined in each of these conditions. The side of a gate that a cysteine was on was inferred from the ratio of the rate constants for the reactions with extracellular reagent in the presence and absence of ACh, divided by the ratio of the rate constants for the reactions with intracellular reagent in the presence and absence of ACh. In the resting state of the receptor, there is a barrier to these reagents between positions –3′ and 2′; in the open state, this barrier is removed. The resting gate is therefore in the same narrow region of the channel that contains the intermediate ring of charge and the selectivity filter.

Desensitization gate. The gate was located in the slow-onset desensitized state using a similar approach[124]. The occluded residues in the desensitized state included the residues between positions –3′ and 9′. So, the desensitization gate is an extension of the resting gate M2 (FIG. 6). The five leucines at position 9′ in $(\alpha7)_5$ were proposed to form the desensitization gate (as opposed to the resting gate)[70]. The SCAM results are consistent with Leu9′ forming the upper bound of the desensitization gate, but not the entire gate, because cysteines at –3′ and –2′ were relatively unreactive in the desensitized state towards intracellularly added reagent[124].

A hydrophobic photolabel, 3-trifluoromethyl-3-(*m*-iodophenyl)diazirine (TID), reacted in the resting state with residues at the 9′ and 13′ positions in βM2 and δM2, and with at the 2′ and 6′ positions in the desensitized state[136,137]. These results are evidence for a resting gate aligned with 9′. However, these results are also consistent with the possibility that TID intercalates into clusters of hydrophobic side chains, that the side chains at 9′ and 13′ are packed into the hydrophobic channel wall in the resting state, and that the side chains at 2′ and 6′ are in the hydrophobic environment of the desensitization gate in the desensitized state (FIG. 6). The effects on the EC_{50} for ACh of mutations of Leu9′ and Val13′ to more polar residues are consistent with these residues being in a nonpolar environment in the resting state, and in a more polar environment in the open state[70,101,138,141]. Furthermore, cysteines that substitute for Leu9′ and Val13′ are much more reactive towards charged reagents in the open state, consistent with their greater exposure in the channel in the open state[101,132].

Auerbach and Akk[30] postulated that there are two separate gates in the channel, the activation gate (here called the resting gate) and the desensitization gate. They proposed that in the resting state, the resting gate is closed and the desensitization gate is open, and that in the agonist-occupied desensitized state, the resting gate is

open and the desensitization gate is closed. They applied their analysis to the fast-onset desensitized state, which occurs on the timescale of 0.1–1 s. The SCAM results were obtained in the stable, slow-onset desensitized state, in which the extent of the channel occlusion could be different from that in the fast-onset desensitized state. Nevertheless, the SCAM results support the idea of non-identical gate structures in the resting and desensitized states, if not entirely separate gate structures.

Concluding remarks

For many years, we have been groping around the ACh receptor and have learned a great many interesting things about it. Now that a high-resolution structure has been obtained, it is as if a light has been turned on. Reassuringly, there are no big surprises. The groping was slow, but effective and necessary for the interpretation of the new structure. Wonderfully concrete as it is, the new structure is just a step in the right direction: it is the structure of a truncated homologue of the ACh receptor. A high-resolution structure of an ACh receptor extracellular domain would be a next step. Of course, the prize would be a structure of the entire receptor, including the channel and the cytoplasmic domain. Much progress has been made by examining crystalline arrays of the receptor by electron microscopy, and perhaps a high-resolution structure will emerge from this approach. However, while waiting for the crystals to grow, we should continue to pursue the questions that the indirect approaches can be used to address. What is the arrangement of the membrane-spanning segments in the subunits? Which segments interact across the different subunit interfaces? Are these different in the different functional states? What are the crucial moving parts for function? We should settle to the satisfaction of everyone the location and nature of the gates. I look forward to much more enlightenment.

1. Langley, J. N. On the contraction of muscle chiefly in relation to the presence of receptive substances. Part 1. *J. Physiol. (Lond.)* **36**, 347–384 (1907).
2. Katz, B. & Thesleff, S. A study of 'desensitization' produced by acetylcholine at the motor end-plate. *J. Physiol. (Lond.)* **138**, 63–80 (1957).
3. Kao, P. N. & Karlin, A. Acetylcholine receptor binding site contains a disulfide cross-link between adjacent half-cystinyl residues. *J. Biol. Chem.* **261**, 8085–8088 (1986).
4. Karlin, A. & Akabas, M. H. Toward a structural basis for the function of nicotinic acetylcholine receptors and their cousins. *Neuron* **15**, 1231–1244 (1995).
5. Ortells, M. O. & Lunt, G. G. Evolutionary history of the ligand-gated ion-channel superfamily of receptors. *Trends Neurosci.* **18**, 121–127 (1995).
6. Tsunoyama, K. & Gojobori, T. Evolution of nicotinic acetylcholine receptor subunits. *Mol. Biol. Evol.* **15**, 518–527 (1998).
7. Cully, D. F. *et al.* Cloning an avermectin-sensitive glutamate-gated chloride channel from *Caenorhabditis elegans*. *Nature* **371**, 707–711 (1994).
8. Zheng, Y. *et al.* Identification of two novel *Drosophila melanogaster* histamine-gated chloride channel subunits expressed in the eye. *J. Biol. Chem.* **277**, 2000–2005 (2002).
9. Reynolds, J. A. & Karlin, A. Molecular weight in detergent solution of acetylcholine receptor from *Torpedo californica*. *Biochemistry* **17**, 2035–2038 (1978).
10. Mishina, M. *et al.* Molecular distinction between fetal and adult forms of muscle acetylcholine receptor. *Nature* **321**, 406–411 (1986).
11. Anand, R., Conroy, W. G., Schoepfer, R., Whiting, P. & Lindstrom, J. Neuronal nicotinic acetylcholine receptors expressed in *Xenopus* oocytes have a pentameric quaternary structure. *J. Biol. Chem.* **266**, 11192–11198 (1991).
12. Cooper, E., Couturier, S. & Ballivet, M. Pentameric structure and subunit stoichiometry of a neuronal nicotinic acetylcholine receptor. *Nature* **350**, 235–238 (1991).
13. Elgoyhen, A. B., Johnson, D. S., Boulter, J., Vetter, D. E. & Heinemann, S. α9: an acetylcholine receptor with novel pharmacological properties expressed in rat cochlear hair cells. *Cell* **79**, 705–715 (1994).
14. Gotti, C. *et al.* Pharmacology and biophysical properties of α7 and α7–α8 α-bungarotoxin receptor subtypes immunopurified from the chick optic lobe. *Eur. J. Neurosci.* **6**, 1281–1291 (1994).
15. Vernallis, A. B., Conroy, W. G. & Berg, D. K. Neurons assemble acetylcholine receptors with as many as three kinds of subunits while maintaining subunit segregation among receptor subtypes. *Neuron* **10**, 451–464 (1993).
16. Le Novere, N., Zoli, M. & Changeux, J. P. Neuronal nicotinic receptor α6 subunit mRNA is selectively concentrated in catecholaminergic nuclei of the rat brain. *Eur. J. Neurosci.* **8**, 2428–2439 (1996).
17. Ramirez-Latorre, J. *et al.* Functional contributions of α5 subunit to neuronal acetylcholine receptor channels. *Nature* **380**, 347–351 (1996).
18. Elgoyhen, A. B. *et al.* α10: a determinant of nicotinic cholinergic receptor function in mammalian vestibular and cochlear mechanosensory hair cells. *Proc. Natl Acad. Sci. USA* **98**, 3501–3506 (2001).
19. Karlin, A. *et al.* The arrangement of the subunits of the acetylcholine receptor of *Torpedo californica*. *J. Biol. Chem.* **258**, 6678–6681 (1983).
20. Stroud, R. M., McCarthy, M. P. & Shuster, M. Nicotinic acetylcholine receptor superfamily of ligand-gated ion channels. *Biochemistry* **29**, 11009–11023 (1990).
21. Unwin, N. Nicotinic acetylcholine receptor at 9 Å resolution. *J. Mol. Biol.* **229**, 1101–1124 (1993).
22. Miyazawa, A., Fujiyoshi, Y., Stowell, M. & Unwin, N. Nicotinic acetylcholine receptor at 4.6 Å resolution: transverse tunnels in the channel wall. *J. Mol. Biol.* **288**, 765–786 (1999).
23. Sakmann, B., Patlak, J. & Neher, E. Single acetylcholine-activated channels show burst-kinetics in presence of desensitizing concentrations of agonist. *Nature* **286**, 71–73 (1980).
24. Neubig, R. R., Boyd, N. D. & Cohen, J. B. Conformations of *Torpedo* acetylcholine receptor associated with ion transport and desensitization. *Biochemistry* **21**, 3460–3467 (1982).
25. Heidmann, T., Bernhardt, J., Neumann, E. & Changeux, J. P. Rapid kinetics of agonist-binding and permeability response analyzed in parallel on acetylcholine receptor rich membranes from *Torpedo marmorata*. *Biochemistry* **22**, 5452–5459 (1983).
26. Jackson, M. B. Perfection of a synaptic receptor: kinetics and energetics of the acetylcholine receptor. *Proc. Natl Acad. Sci. USA* **86**, 2199–2203 (1989).
27. Auerbach, A. A statistical analysis of acetylcholine receptor activation in *Xenopus* myocytes: stepwise versus concerted models of gating. *J. Physiol. (Lond.)* **461**, 339–378 (1993).
28. Hess, G. Determination of the chemical mechanism of neurotransmitter receptor-mediated reaction by rapid chemical kinetic techniques. *Biochemistry* **32**, 989–1000 (1993).
29. Edelstein, S. J., Schaad, O., Henry, E., Bertrand, D. & Changeux, J. P. A kinetic mechanism for nicotinic acetylcholine receptors based on multiple allosteric transitions. *Biol. Cybern.* **75**, 361–379 (1996).
30. Auerbach, A. & Akk, G. Desensitization of mouse nicotinic acetylcholine receptor channels. A two-gate mechanism. *J. Gen. Physiol.* **112**, 181–197 (1998).
A thorough single-channel analysis of the fast phase of desensitization finds that the receptor desensitizes most readily from the open state and, as first shown in reference 2, returns to the resting state without opening. The authors propose an interesting model in which there are separate resting and desensitization gates that are alternately open and closed, the interaction of which determines the kinetics of desensitization and recovery.
31. Prince, R. J. & Sine, S. M. Acetylcholine and epibatidine binding to muscle acetylcholine receptors distinguish between concerted and uncoupled models. *J. Biol. Chem.* **274**, 19623–19629 (1999).
The ACh-binding sites seem to switch independently between functional states, generating asymmetrical states, contrary to the MWC postulate of concerted transitions.
32. Reitstetter, R., Lukas, R. J. & Gruener, R. Dependence of nicotinic acetylcholine receptor recovery from desensitization on the duration of agonist exposure. *J. Pharmacol. Exp. Ther.* **289**, 656–660 (1999).
33. Grosman, C. & Auerbach, A. The dissociation of acetylcholine from open nicotinic receptor channels. *Proc. Natl Acad. Sci. USA* **98**, 14102–14107 (2001).
This is another searching analysis of receptor kinetics from Auerbach's laboratory, which expands the work of reference 30. This one estimates the rate constants for the association and dissociation of agonist from the open state, and yields the theoretically expected result that the much higher affinity of agonist for the open state than for the resting state drives activation.
34. Jones, M. V. & Westbrook, G. L. The impact of receptor desensitization on fast synaptic transmission. *Trends Neurosci.* **19**, 96–101 (1996).
35. Monod, J., Wyman, J. & Changeux, J.-P. On the nature of allosteric transitions: a plausible model. *J. Mol. Biol.* **12**, 88–118 (1965).
36. Changeux, J.-P., Thiery, J., Tung, Y. & Kittel, C. On the cooperativity of biological membranes. *Proc. Natl Acad. Sci. USA* **57**, 335–341 (1967).
37. Karlin, A. On the application of 'a plausible model' of allosteric proteins to the receptor for acetylcholine. *J. Theor. Biol.* **16**, 306–320 (1967).
38. Kawai, H., Cao, L., Dunn, S. M., Dryden, W. F. & Raftery, M. A. Interaction of a semirigid agonist with *Torpedo* acetylcholine receptor. *Biochemistry* **39**, 3867–3876 (2000).
39. Krauss, M., Korr, D., Herrmann, A. & Hucho, F. Binding properties of agonists and antagonists to distinct allosteric states of the nicotinic acetylcholine receptor are incompatible with a concerted model. *J. Biol. Chem.* **275**, 30196–30201 (2000).
40. Brejc, K. *et al.* Crystal structure of an ACh-binding protein reveals the ligand-binding domain of nicotinic receptors. *Nature* **411**, 269–276 (2001).
The structure of the snail AChBP is solved, illuminating 30 years of research on the ACh receptor and other Cys-loop receptors, and uncovering fascinating details that only a high-resolution structure can provide.
41. Smit, A. B. *et al.* A glia-derived acetylcholine-binding protein that modulates synaptic transmission. *Nature* **411**, 261–268 (2001).
The discovery and properties of the snail AChBP are described, and evidence is presented that this protein, secreted by snail glia, has an unusual role in shaping neurotransmission by acetylcholine in snail synapses.
42. Ratnam, M. *et al.* Location of antigenic determinants on primary sequences of subunits of nicotinic acetylcholine receptor by peptide mapping. *Biochemistry* **25**, 2621–2632 (1986).
43. Le Novere, N., Corringer, P. J. & Changeux, J. P. Improved secondary structure predictions for a nicotinic receptor subunit: incorporation of solvent accessibility and experimental data into a two-dimensional representation. *Biophys. J.* **76**, 2329–2345 (1999).

This paper provides a paradigm for integrating the outputs of several prediction programs to obtain a consensus secondary structure for members of a protein family. Judging by the subsequently solved structure of the homologous AChBP, the prediction was remarkably good.

44. Karlin, A. Explorations of the nicotinic acetylcholine receptor. *Harvey Lect.* **85**, 71–107 (1991).
45. Reiter, M. J., Cowburn, D. A., Prives, J. M. & Karlin, A. Affinity labeling of the acetylcholine receptor in the electroplax: electrophoretic separation in sodium dodecyl sulfate. *Proc. Natl Acad. Sci. USA* **69**, 1168–1172 (1972).
46. Kao, P. N. *et al.* Identification of the α subunit half-cystine specifically labeled by an affinity reagent for the acetylcholine receptor binding site. *J. Biol. Chem.* **259**, 11662–11665 (1984).
47. Galzi, J.-L. *et al.* Identification of a novel amino acid α-tyrosine 93 within the cholinergic ligand-binding sites of the acetylcholine receptor by photolabeling. Additional evidence for a three-loop model of the cholinergic ligand-binding site. *J. Biol. Chem.* **265**, 10430–10437 (1990).
48. Middleton, R. E. & Cohen, J. B. Mapping of the acetylcholine binding site of the nicotinic acetylcholine receptor: [^{3}H]nicotine as an agonist photoaffinity label. *Biochemistry* **30**, 6987–6997 (1991).
49. Kurosaki, T. *et al.* Functional properties of nicotinic acetylcholine receptor subunits expressed in various combinations. *FEBS Lett.* **214**, 253–258 (1987).
50. Blount, P. & Merlie, J. P. Molecular basis of the two nonequivalent ligand binding sites of the muscle nicotinic acetylcholine receptor. *Neuron* **3**, 349–357 (1989).
51. Sine, S. M. & Claudio, T. γ- and δ-subunits regulate the affinity and the cooperativity of ligand binding to the acetylcholine receptor. *J. Biol. Chem.* **266**, 19369–19377 (1991).
52. Sine, S. M. Molecular dissection of subunit interfaces in the acetylcholine receptor: identification of residues that determine curare selectivity. *Proc. Natl Acad. Sci. USA* **90**, 9436–9440 (1993).
53. Wang, D., Chiara, D. C., Xie, Y. & Cohen, J. B. Probing the structure of the nicotinic acetylcholine receptor with 4-benzoylbenzoylcholine, a novel photoaffinity competitive antagonist. *J. Biol. Chem.* **275**, 28666–28674 (2000).
54. Czajkowski, C. & Karlin, A. Structure of the nicotinic receptor acetylcholine-binding site. Identification of acidic residues in the δ subunit within 0.9 nm of the α subunit binding site disulfide. *J. Biol. Chem.* **270**, 3160–3164 (1995).
55. Pedersen, S. E. & Cohen, J. B. D-Tubocurarine binding sites are located at α–γ and α–δ subunit interfaces of the nicotinic acetylcholine receptor. *Proc. Natl Acad. Sci. USA* **87**, 2785–2789 (1990).
56. Czajkowski, C. & Karlin, A. Agonist binding site of *Torpedo* electric tissue nicotinic acetylcholine receptor. A negatively charged region of the δ subunit within 0.9 nm of the α subunit binding site disulfide. *J. Biol. Chem.* **266**, 22603–22612 (1991).
57. Machold, J. *et al.* Photolabeling reveals the proximity of the α-neurotoxin binding site to the M2 helix of the ion channel in the nicotinic acetylcholine receptor. *Proc. Natl Acad. Sci. USA* **92**, 7282–7286 (1995).
58. Zhong, W. *et al.* From *ab initio* quantum mechanics to molecular neurobiology: a cation–π binding site in the nicotinic receptor. *Proc. Natl Acad. Sci. USA* **95**, 12088–12093 (1998).
59. Schmitt, J. D., Sharples, C. G. & Caldwell, W. S. Molecular recognition in nicotinic acetylcholine receptors: the importance of π–cation interactions. *J. Med. Chem.* **42**, 3066–3074 (1999).
60. Martin, M. D. & Karlin, A. Functional effects on the acetylcholine receptor of multiple mutations of γAsp174 and δAsp180. *Biochemistry* **36**, 10742–10750 (1997).
61. Akk, G., Zhou, M. & Auerbach, A. A mutational analysis of the acetylcholine receptor channel transmitter binding site. *Biophys. J.* **76**, 207–218 (1999).
62. Stauffer, D. A. & Karlin, A. Electrostatic potential of the acetylcholine binding sites in the nicotinic receptor probed by reactions of binding-site cysteines with charged methanethiosulfonates. *Biochemistry* **33**, 6840–6849 (1994).
63. Osaka, H., Sugiyama, N. & Taylor, P. Distinctions in agonist and antagonist specificity conferred by anionic residues of the nicotinic acetylcholine receptor. *J. Biol. Chem.* **273**, 12758–12765 (1998).
64. Karlin, A. Chemical modification of the active site of the acetylcholine receptor. *J. Gen. Physiol.* **54**, 245S–264S (1969).
65. Sullivan, D. A. & Cohen, J. B. Mapping the agonist binding site of the nicotinic acetylcholine receptor. Orientation requirements for activation by covalent agonist. *J. Biol. Chem.* **275**, 12651–12660 (2000).
66. Cohen, J. B., Sharp, S. D. & Liu, W. S. Structure of the agonist-binding site of the nicotinic acetylcholine receptor. [^{3}H]Acetylcholine mustard identifies residues in the cation-binding subsite. *J. Biol. Chem.* **266**, 23354–23364 (1991).
67. Armstrong, N. & Gouaux, E. Mechanisms for activation and antagonism of an AMPA-sensitive glutamate receptor: crystal structures of the GluR2 ligand binding core. *Neuron* **28**, 165–181 (2000).
The structure of the ligand-binding portion of the extracellular domain of a glutamate receptor (not a Cys-loop receptor) was solved to high resolution. This paper shows that ligands induce a graded change in this structure depending on their effectiveness as an activator.
68. Damle, V. N. & Karlin, A. Effects of agonists and antagonists on the reactivity of the binding site disulfide in acetylcholine receptor from *Torpedo californica*. *Biochemistry* **19**, 3924–3932 (1980).
69. Steinbach, J. H. & Chen, Q. Antagonist and partial agonist actions of D-tubocurarine at mammalian muscle acetylcholine receptors. *J. Neurosci.* **15**, 230–240 (1995).
70. Revah, F. *et al.* Mutations in the channel domain alter desensitization of a neuronal nicotinic receptor. *Nature* **353**, 846–849 (1991).
71. Mishina, M. *et al.* Location of functional regions of acetylcholine receptor α-subunit by site directed mutagenesis. *Nature* **313**, 364–369 (1985).
72. Galzi, J. L. *et al.* Functional significance of aromatic amino acids from three peptide loops of the α7 neuronal nicotinic receptor site investigated by site-directed mutagenesis. *FEBS Lett.* **294**, 198–202 (1991).
73. Sine, S. M., Quiram, P., Papanikolaou, F., Kreienkamp, H. J. & Taylor, P. Conserved tyrosines in the α subunit of the nicotinic acetylcholine receptor stabilize quaternary ammonium groups of agonists and curariform antagonists. *J. Biol. Chem.* **269**, 8808–8816 (1994).
74. Tomaselli, G. F., McLaughlin, J. T., Jurman, M. E., Hawrot, E. & Yellen, G. Mutations affecting agonist sensitivity of the nicotinic acetylcholine receptor. *Biophys. J.* **60**, 721–727 (1991).
75. O'Leary, M. E., Filatov, G. N. & White, M. M. Characterization of D-tubocurarine binding site of *Torpedo* acetylcholine receptor. *Am. J. Physiol.* **266**, C648–C653 (1994).
76. Xie, Y. & Cohen, J. B. Contributions of *Torpedo* nicotinic acetylcholine receptor γTrp-55 and δTrp-57 to agonist and competitive antagonist function. *J. Biol. Chem.* **276**, 2417–2426 (2001).
These tryptophan residues were the first non-α-subunit residues to be identified that contribute to the ACh-binding site. The properties of mutants in these residues provide insight into the asymmetry of the binding sites and the induction of conformational change by the binding of (+)-tubocurarine.
77. Sine, S. M., Kreienkamp, H. J., Bren, N., Maeda, R. & Taylor, P. Molecular dissection of subunit interfaces in the acetylcholine receptor: identification of determinants of α-conotoxin M1 selectivity. *Neuron* **15**, 205–211 (1995).
78. Chiara, D. C., Xie, Y. & Cohen, J. B. Structure of the agonist-binding sites of the *Torpedo* nicotinic acetylcholine receptor: affinity-labeling and mutational analyses identify γTyr-111/δArg-113 as antagonist affinity determinants. *Biochemistry* **38**, 6689–6698 (1999).
79. Sine, S. M. Identification of equivalent residues in the γ, δ, and ε subunits of the nicotinic receptor that contribute to α-bungarotoxin binding. *J. Biol. Chem.* **272**, 23521–23527 (1997).
80. Damle, V. N. & Karlin, A. Affinity labeling of one of two α-neurotoxin binding sites in acetylcholine receptor from *Torpedo californica*. *Biochemistry* **17**, 2039–2045 (1978).
81. Martinez, K. L., Corringer, P. J., Edelstein, S. J., Changeux, J. P. & Mérola, F. Structural differences in the two agonist binding sites of the *Torpedo* nicotinic acetylcholine receptor revealed by time-resolved fluorescence spectroscopy. *Biochemistry* **39**, 6979–6990 (2000).
82. McArdle, J. J. *et al.* Waglerin-1 selectively blocks the epsilon form of the muscle nicotinic acetylcholine receptor. *J. Pharmacol. Exp. Ther.* **289**, 543–550 (1999).
83. Molles, B. E. *et al.* Identification of residues at the α and ε subunit interfaces mediating species selectivity of Waglerin-1 for nicotinic acetylcholine receptors. *J. Biol. Chem.* 27 November 2001 [epub ahead of print].
84. Osaka, H., Malany, S., Molles, B. E., Sine, S. M. & Taylor, P. Pairwise electrostatic interactions between α-neurotoxins and γ, δ, and ε subunits of the nicotinic acetylcholine receptor. *J. Biol. Chem.* **275**, 5478–5484 (2000).
85. Edelstein, S. & Changeux, J. P. Allosteric transitions of the acetylcholine receptor. *Adv. Protein Chem.* **51**, 121–184 (1998).
86. Lee, C. Y. Chemistry and pharmacology of polypeptide toxins in snake venoms. *Annu. Rev. Pharmacol.* **12**, 265–286 (1972).
87. Changeux, J. P., Kasai, M. & Lee, C. Y. Use of a snake venom toxin to characterize the cholinergic receptor protein. *Proc. Natl Acad. Sci. USA* **67**, 1241–1247 (1970).
88. Miledi, R., Molinoff, P. & Potter, L. T. Isolation of the cholinergic receptor protein of *Torpedo* electric tissue. *Nature* **229**, 554–557 (1971).
89. Tsetlin, V. Snake venom α-neurotoxins and other 'three-finger' proteins. *Eur. J. Biochem.* **264**, 281–286 (1999).
90. Haggerty, J. G. & Froehner, S. C. Restoration of ^{125}I-α-bungarotoxin binding activity to the α subunit of *Torpedo* acetylcholine receptor isolated by gel electrophoresis in sodium dodecyl sulfate. *J. Biol. Chem.* **256**, 8294–8297 (1981).
91. Wilson, P. T., Lentz, T. L. & Hawrot, E. Determination of the primary amino acid sequence specifying the α-bungarotoxin binding site on the α subunit of the acetylcholine receptor from *Torpedo californica*. *Proc. Natl Acad. Sci. USA* **82**, 8790–8794 (1985).
92. Neumann, D., Barchan, D., Safran, A., Gershoni, J. M. & Fuchs, S. Mapping of the α-bungarotoxin binding site within the α subunit of the acetylcholine receptor. *Proc. Natl Acad. Sci. USA* **83**, 3008–3011 (1986).
93. Samson, A. O., Chill, J. H., Rodriguez, E., Scherf, T. & Anglister, J. NMR mapping and secondary structure determination of the major acetylcholine receptor α-subunit determinant interacting with α-bungarotoxin. *Biochemistry* **40**, 5464–5473 (2001).
94. Harel, M. *et al.* The binding site of acetylcholine receptor as visualized in the X-ray structure of a complex between α-bungarotoxin and a mimotope peptide. *Neuron* **32**, 173–174 (2001).
A remarkable tale is told of the development of a short synthetic peptide with high affinity for α-bungarotoxin, the crystallization of the complex, and the superposition of the structure on the AChBP. By homology, this reveals the mode of binding of the snake α-neurotoxins to the ACh receptor.
95. Kreienkamp, H. J., Sine, S. M., Maeda, R. K. & Taylor, P. Glycosylation sites selectively interfere with α-toxin binding to the nicotinic acetylcholine receptor. *J. Biol. Chem.* **269**, 8108–8114 (1994).
96. Antil, S., Servent, D. & Menez, A. Variability among the sites by which curaremimetic toxins bind to *Torpedo* acetylcholine receptor, as revealed by identification of the functional residues of α-cobratoxin. *J. Biol. Chem.* **274**, 34851–34858 (1999).
97. Spura, A. *et al.* Biotinylation of substituted cysteines in the nicotinic acetylcholine receptor reveals distinct binding modes for α-bungarotoxin and erabutoxin a. *J. Biol. Chem.* **275**, 22452–22460 (2000).
98. Spura, A. *et al.* Probing the agonist domain of the nicotinic acetylcholine receptor by cysteine scanning mutagenesis reveals residues in proximity to the α-bungarotoxin binding site. *Biochemistry* **38**, 4912–4921 (1999).
99. Gorne-Tschelnokow, U., Strecker, A., Kaduk, C., Naumann, D. & Hucho, F. The transmembrane domains of the nicotinic acetylcholine receptor contain α-helical and β structures. *EMBO J.* **13**, 338–341 (1994).
100. Methot, N., Ritchie, B. D., Blanton, M. P. & Baenziger, J. E. Structure of the pore-forming transmembrane domain of a ligand-gated ion channel. *J. Biol. Chem.* **276**, 23726–23732 (2001).
101. Akabas, M. H., Kaufmann, C., Archdeacon, P. & Karlin, A. Identification of acetylcholine receptor channel-lining residues in the entire M2 segment of the α subunit. *Neuron* **13**, 919–927 (1994).
102. Zhang, H. & Karlin, A. Contribution of the β subunit M2 segment to the ion-conducting pathway of the acetylcholine receptor. *Biochemistry* **37**, 7952–7964 (1998).
The application of SCAM to 104 cysteine-substitution mutants of two membrane-spanning segments of two ACh receptor subunits is summarized. The modification of one of the mutants causes the appearance of multiple single-channel subconductance states and channel lifetimes.
103. Akabas, M. H. & Karlin, A. Identification of acetylcholine receptor channel-lining residues in the M1 segment of the α subunit. *Biochemistry* **34**, 12496–12500 (1995).
104. Zhang, H. & Karlin, A. Identification of acetylcholine receptor channel-lining residues in the M1 segment of the β subunit. *Biochemistry* **36**, 15856–15864 (1997).
105. Blanton, M. P. & Cohen, J. B. Identifying the lipid–protein interface of the *Torpedo* nicotinic acetylcholine receptor: secondary structure implication. *Biochemistry* **33**, 2859–2872 (1994).
106. Blanton, M. P., Dangott, L. J., Raja, S. K., Lala, A. K. & Cohen, J. B. Probing the structure of the nicotinic acetylcholine receptor ion channel with the uncharged photoactivable compound [^{3}H]-diazofluorene. *J. Biol. Chem.* **273**, 8659–8668 (1998).
107. Claudio, T., Ballivet, M., Patrick, J. & Heinemann, S. Nucleotide and deduced amino acid sequences of *Torpedo californica* acetylcholine receptor γ subunit. *Proc. Natl Acad. Sci. USA* **80**, 1111–1115 (1983).

108. Devillers-Thiery, A., Giraudat, J., Bentaboulet, M. & Changeux, J.-P. Complete mRNA coding sequence of the acetylcholine binding α subunit of *Torpedo marmorata* acetylcholine receptor: a model for the transmembrane organization of the polypeptide chain. *Proc. Natl Acad. Sci. USA* **80**, 2067–2071 (1983).
109. Noda, M. *et al.* Structural homology of *Torpedo californica* acetylcholine receptor subunits. *Nature* **302**, 528–532 (1983).
110. Tamamizu, S. *et al.* Functional effects of periodic tryptophan substitutions in the α M4 transmembrane domain of the *Torpedo californica* nicotinic acetylcholine receptor. *Biochemistry* **39**, 4666–4673 (2000).
111. Hille, B. *Ionic Channels of Excitable Membranes* (Sinauer Associates, Sunderland, Massachusetts, 1992).
112. Sakmann, B. Nobel Lecture. Elementary steps in synaptic transmission revealed by currents through single ion channels. *Neuron* **8**, 613–629 (1992).
113. Dani, J. A. Open channel structure and ion binding sites of the nicotinic acetylcholine receptor channel. *J. Neurosci.* **9**, 884–892 (1989).
114. Eisenberg, R. Computing the field in proteins and channels. *J. Membr. Biol.* **150**, 1–25 (1996).
115. Green, M. E. & Lu, J. Monte-Carlo simulation of the effects of charges on water and ions in a tapered pore. *J. Colloid Interface Sci.* **171**, 117–126 (1995).
116. Morais-Cabral, J. H., Zhou, Y. & MacKinnon, R. Energetic optimization of ion conduction rate by the K^+ selectivity filter. *Nature* **414**, 37–42 (2001).
117. Zhou, Y., Morais-Cabral, J. H., Kaufman, A. & MacKinnon, R. Chemistry of ion coordination and hydration revealed by a K^+ channel–Fab complex at 2.0 Å resolution. *Nature* **414**, 43–48 (2001).
In references 116 and 117, the mechanism of ion conduction in a K^+ channel is revealed in exquisite detail. These papers should be avoided by the envious.
118. Villarroel, A., Herlitze, S., Koenen, M. & Sakmann, B. Location of a threonine residue in the α-subunit M2 transmembrane segment that determines the ion flow through the acetylcholine receptor channel. *Proc. R. Soc. Lond. B* **243**, 69–74 (1991).
119. Konno, T. *et al.* Rings of anionic amino acids as structural determinants of ion selectivity in the acetylcholine receptor channel. *Proc. R. Soc. Lond. B* **244**, 69–79 (1991).
120. Imoto, K. *et al.* A ring of uncharged polar amino acids as a component of channel constriction in the nicotinic acetylcholine receptor. *FEBS Lett.* **289**, 193–200 (1991).
121. Cohen, B. N., Labarca, C., Davidson, N. & Lester, H. A. Mutations in M2 alter the selectivity of the mouse nicotinic acetylcholine receptor for organic and alkali metal cations. *J. Gen. Physiol.* **100**, 373–400 (1992).
122. Corringer, P. J. *et al.* Mutational analysis of the charge selectivity filter of the α7 nicotinic acetylcholine receptor. *Neuron* **22**, 831–843 (1999).
By painstaking alterations in the sequence of M2, the authors determine the necessary and sufficient conditions for switching from cation and to anion selectivity. The result is amazing and somewhat mysterious.
123. Wilson, G. G. & Karlin, A. The location of the gate in the acetylcholine receptor channel. *Neuron* **20**, 1269–1281 (1998).
A new approach to locating a gate is applied to the ACh receptor, and the result is controversial.
124. Wilson, G. G. & Karlin, A. Acetylcholine channel structure in the resting, open, and desensitized states probed with the substituted-cysteine-accessibility method. *Proc. Natl Acad. Sci. USA* **98**, 1241–1248 (2001).
Widespread differences in the structure of M2 in the different states of the receptor are rationalized in terms of gating and gates.
125. Imoto, K. *et al.* Location of a δ-subunit region determining ion transport through the acetylcholine receptor channel. *Nature* **324**, 670–674 (1986).
126. Imoto, K. *et al.* Rings of negatively charged amino acids determine the acetylcholine receptor channel conductance. *Nature* **335**, 645–648 (1988).
127. Giraudat, J., Dennis, M., Heidmann, T., Chang, J.-Y. & Changeux, J.-P. Structure of the high-affinity binding site for noncompetitive blockers of the acetylcholine receptor: serine-262 of the δ subunit is labeled by [^{3}H]chlorpromazine. *Proc. Natl Acad. Sci. USA* **83**, 2719–2723 (1986).
128. Giraudat, J. *et al.* Structure of the high-affinity binding site for noncompetitive blockers of the acetylcholine receptor: [^{3}H]chlorpromazine labels homologous residues in the β and δ chains. *Biochemistry* **26**, 2410–2418 (1987).
129. Hucho, F., Oberthur, W. & Lottspeich, F. The ion channel of the nicotinic acetylcholine receptor is formed by the homologous helices M II of the receptor subunits. *FEBS Lett.* **205**, 137–142 (1986).
130. DiPaola, M., Kao, P. N. & Karlin, A. Mapping the α-subunit site photolabeled by the noncompetitive inhibitor [^{3}H]quinacrine azide in the active state of the nicotinic acetylcholine receptor. *J. Biol. Chem.* **265**, 11017–11029 (1990).
131. Akabas, M. H., Stauffer, D. A., Xu, M. & Karlin, A. Acetylcholine receptor channel structure probed in cysteine-substitution mutants. *Science* **258**, 307–310 (1992).
132. Pascual, J. M. & Karlin, A. State-dependent accessibility and electrostatic potential in the channel of the acetylcholine receptor: inferences from rates of reaction of thiosulfonates with substituted cysteines in the M2 segment of the α subunit. *J. Gen. Physiol.* **111**, 717–739 (1998).
133. Wilson, G. G., Pascual, J. M., Brooijmans, N., Murray, D. & Karlin, A. The intrinsic electrostatic potential and the intermediate ring of charge in the acetylcholine receptor channel. *J. Gen. Physiol.* **115**, 93–106 (2000).
134. Heidmann, T. & Changeux, J. P. Time-resolved photolabeling by the noncompetitive blocker chlorpromazine of the acetylcholine receptor in its transiently open and closed ion channel conformations. *Proc. Natl Acad. Sci. USA* **81**, 1897–1901 (1984).
135. Cox, R. N., Kaldany, R. R., DiPaola, M. & Karlin, A. Time-resolved photolabeling by quinacrine azide of a noncompetitive inhibitor site of the nicotinic acetylcholine receptor in a transient, agonist-induced state. *J. Biol. Chem.* **260**, 7186–7193 (1985).
136. White, B. H. & Cohen, J. B. Agonist-induced changes in the structure of the acetylcholine receptor M2 regions revealed by photoincorporation of an uncharged nicotinic noncompetitive antagonist. *J. Biol. Chem.* **267**, 15770–15783 (1992).
137. McCarthy, M. P. & Moore, M. A. Effects of lipids and detergents on the conformation of the nicotinic acetylcholine receptor from *Torpedo californica*. *J. Biol. Chem.* **267**, 7655–7663 (1992).
138. Bertrand, D., Galzi, J. L., Devillers-Thiery, A., Bertrand, S. & Changeux, J. P. Mutations at two distinct sites within the channel domain M2 alter calcium permeability of neuronal α7 nicotinic receptor. *Proc. Natl Acad. Sci. USA* **90**, 6971–6975 (1993).
139. Labarca, C. *et al.* Channel gating governed symmetrically by conserved leucine residues in the M2 domain of nicotinic receptors. *Nature* **376**, 514–516 (1995).
140. Filatov, G. N. & White, M. M. The role of conserved leucines in the M2 domain of the acetylcholine receptor in channel gating. *Mol. Pharmacol.* **48**, 379–384 (1995).
141. Kosolapov, A. V., Filatov, G. N. & White, M. M. Acetylcholine receptor gating is influenced by the polarity of amino acids at position 9′ in the M2 domain. *J. Membr. Biol.* **174**, 191–197 (2000).
142. Grosman, C. & Auerbach, A. Asymmetric and independent contribution of the second transmembrane segment 12′ residues to diliganded gating of acetylcholine receptor channels: a single-channel study with choline as the agonist. *J. Gen. Physiol.* **115**, 637–651 (2000).
143. Grosman, C., Salamone, F. N., Sine, S. M. & Auerbach, A. The extracellular linker of muscle acetylcholine receptor channels is a gating control element. *J. Gen. Physiol.* **116**, 327–340 (2000).
144. Wang, H. L. *et al.* Acetylcholine receptor M3 domain: stereochemical and volume contributions to channel gating. *Nature Neurosci.* **2**, 226–233 (1999).
145. Bouzat, C., Barrantes, F. & Sine, S. Nicotinic receptor fourth transmembrane domain: hydrogen bonding by conserved threonine contributes to channel gating kinetics. *J. Gen. Physiol.* **115**, 663–672 (2000).
146. DaCosta, C. J., Ogrel, A. A., McCardy, E. A., Blanton, M. P. & Baenziger, J. E. Lipid–protein interactions at the nicotinic acetylcholine receptor: a functional coupling between nicotinic receptors and phosphatidic acid-containing lipid bilayers. *J. Biol. Chem.* **277**, 201–208 (2002).
The profound effects of the lipid environment on receptor structure and function are reviewed and further shown.
147. Wang, H. L. *et al.* Fundamental gating mechanism of nicotinic receptor channel revealed by mutation causing a congenital myasthenic syndrome. *J. Gen. Physiol.* **116**, 449–462 (2000).
148. Unwin, N. Acetylcholine receptor channel imaged in the open state. *Nature* **373**, 37–43 (1995).
149. Takahama, K. & Klee, M. R. Voltage clamp analysis of the kinetics of piperidine-induced chloride current in isolated *Aplysia* neurons. *Naunyn Schmiedebergs Arch. Pharmacol.* **342**, 575–581 (1990).
150. Kehoe, J. & McIntosh, J. M. Two distinct nicotinic receptors, one pharmacologically similar to the vertebrate α7-containing receptor, mediate Cl currents in *Aplysia* neurons. *J. Neurosci.* **18**, 8198–8213 (1998).
151. Adams, D. J., Dwyer, T. M. & Hille, B. The permeability of endplate channels to monovalent and divalent metal cations. *J. Gen. Physiol.* **75**, 493–510 (1980).
152. Lewis, C. A. & Stevens, C. F. Acetylcholine receptor channel ionic selectivity: ions experience an aqueous environment. *Proc. Natl Acad. Sci. USA* **80**, 6110–6113 (1983).
153. Fieber, L. A. & Adams, D. J. Acetylcholine-evoked currents in cultured neurones dissociated from rat parasympathetic cardiac ganglia. *J. Physiol. (Lond.)* **434**, 215–237 (1991).
154. Vernino, S., Amador, M., Luetje, C. W., Patrick, J. & Dani, J. A. Calcium modulation and high calcium permeability of neuronal nicotinic acetylcholine receptors. *Neuron* **8**, 127–134 (1992).
155. Katz, E. *et al.* High calcium permeability and calcium block of the α9 nicotinic acetylcholine receptor. *Hear. Res.* **141**, 117–128 (2000).
156. Cohen, B. N., Labarca, C., Czyzyk, L., Davidson, N. & Lester, H. A. $Tris^+/Na^+$ permeability ratios of nicotinic acetylcholine receptors are reduced by mutations near the intracellular end of the M2 region. *J. Gen. Physiol.* **99**, 545–572 (1992).
157. Villarroel, A., Herlitze, S., Witzemann, V., Koenen, M. & Sakmann, B. Asymmetry of the rat acetylcholine receptor subunits in the narrow region of the pore. *Proc. R. Soc. Lond. B* **249**, 317–324 (1992).
158. Gunthorpe, M. J. & Lummis, S. C. Conversion of the ion selectivity of the $5\text{-}HT_{3A}$ receptor from cationic to anionic reveals a conserved feature of the ligand-gated ion channel superfamily. *J. Biol. Chem.* **276**, 10977–10983 (2001).
159. Keramidas, A., Moorhouse, A. J., French, C. R., Schofield, P. R. & Barry, P. H. M2 pore mutations convert the glycine receptor channel from being anion- to cation-selective. *Biophys. J.* **79**, 247–259 (2000).
160. Adcock, C., Smith, G. R. & Sansom, M. S. The nicotinic acetylcholine receptor: from molecular model to single-channel conductance. *Eur. Biophys. J.* **29**, 29–37 (2000).
161. Yakel, J. L., Lagrutta, A., Adelman, J. P. & North, R. A. Single amino acid substitution affects desensitization of the 5-hydroxytryptamine type 3 receptor expressed in *Xenopus* oocytes. *Proc. Natl Acad. Sci. USA* **90**, 5030–5033 (1993).
162. Xu, M. & Akabas, M. H. Identification of channel-lining residues in the M2 membrane-spanning segment of the $GABA_A$ receptor α1 subunit. *J. Gen. Physiol.* **107**, 195–205 (1996).
163. Karlin, A. & Akabas, M. H. Substituted-cysteine accessibility method. *Methods Enzymol.* **293**, 123–145 (1998).
164. Javitch, J. A., Li, X., Kaback, J. & Karlin, A. A cysteine residue in the third membrane-spanning segment of the human D2 dopamine receptor is exposed in the binding-site crevice. *Proc. Natl Acad. Sci. USA* **91**, 10355–10359 (1994).
165. Javitch, J. A., Fu, D., Chen, J. & Karlin, A. Mapping the binding-site crevice of the dopamine D2 receptor by the substituted-cysteine accessibility method. *Neuron* **14**, 825–831 (1995).
166. Bruice, T. W. & Kenyon, G. L. Novel alkyl alkanethiosulfonate sulfhydryl reagents. Modification of derivatives of L-cysteine. *J. Protein Chem.* **1**, 47–58 (1982).
167. Roberts, D. D., Lewis, S. D., Ballou, D. P., Olson, S. T. & Shafer, J. A. Reactivity of small thiolate anions and cysteine-25 in papain toward methyl methanethiosulfonate. *Biochemistry* **25**, 5595–5601 (1986).
168. Kaback, H. R. A molecular mechanism for energy coupling in a membrane transport protein, the lactose permease of *Escherichia coli*. *Proc. Natl Acad. Sci. USA* **94**, 5539–5543 (1997).

Online links

DATABASES

The following terms in this article are linked online to:

Entrez Protein: http://www.ncbi.nlm.nih.gov/entrez/
AChBP | α-bungarotoxin | conotoxin MI | erabutoxin

LocusLink: http://www.ncbi.nlm.nih.gov/LocusLink/
α1-subunit | α2–α10 | β1-subunit | β2–β4 | δ-subunit | ε-subunit | γ-subunit | $GABA_A$ receptor | GluR2 | glycine receptors | $5\text{-}HT_3$ receptor

Protein Data Bank: http://www.rcsb.org/pdb/
1FTO: GluR2 S1S2, apo state | 1HC9: α-bungarotoxin, complex with high-affinity peptide | 1I9B: acetylcholine-binding protein (AChBP)

FURTHER INFORMATION

Encyclopedia of Life Sciences: http://www.els.net/
ion channels | nicotinic acetylcholine receptors | nicotinic acetylcholine receptors in muscle | nicotinic acetylcholine receptors in neurons

Families of Transport Proteins:
http://www.biology.ucsd.edu/%7Emsaier/transport/toc.html

Ligand-Gated Ion Channel Database:
http://www.pasteur.fr/recherche/banques/LGIC/LGIC.html

The Ion Channel Web Page:
http://phy025.lubb.ttuhsc.edu/Neely/ionchann.htm

Access to this interactive links box is free online.